ACS Biomaterials SCIENCE & ENGINEERING

pubs.acs.org/journal/abseba

Letter

Toward Antibacterial Coatings for Personalized Implants

F. Jahanmard,[†] F.M. Dijkmans,[†] A. Majed, H.C. Vogely, B.C.H. van der Wal, D.A.C. Stapels, S.M. Ahmadi, T. Vermonden, and S. Amin Yavari*

Cite This: *ACS Biomater. Sci. Eng.* 2020, 6, 5486−5492

Read Online

ACCESS | Metrics & More | Article Recommendations | Supporting Information

ABSTRACT: The complex reconstructive surgeries for which patient-specific orthopedic, maxillofacial, or dental implants are used often necessitate wounds that are open for a considerable amount of time. Unsurprisingly, this allows bacteria to establish implant-associated infection, despite the scrupulous sterilization efforts made during surgery. Here, we developed a prophylactic bactericidal coating via electrophoretic deposition technology for two 3D-printed porous titanium implant designs. The surface characteristics, antibiotic release behavior, antibacterial properties, and impact on osteoblast cell proliferation of the optimized coatings were investigated. The results unequivocally confirmed the biofunctionality of the implants in vitro. This study reveals a new avenue for future antibacterial patient-specific implants.

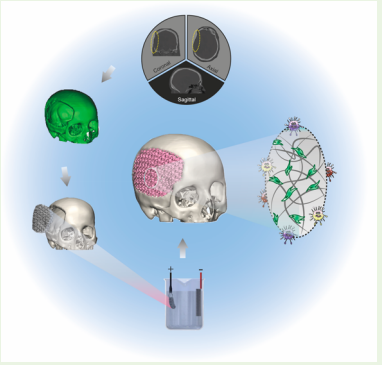

KEYWORDS: *metal 3D printing, antibacterial coating, personalized implants*

An established implant-associated infection (IAI) is often difficult to treat, as bacteria form a biofilm on the implant that hinders the host immune response and hampers antibiotic penetration.[1] By approximation, the killing of biofilm-residing bacteria requires antibiotic concentrations 1000 times higher than needed to kill planktonic bacteria.[2] As compared to systemic treatment, local delivery of antibacterial agents is more likely to result in therapeutic levels at the infection, while reducing the chance of systemic toxic effects. At the same time, there is an increasing demand for patient-specific solutions to repair large and complex bone defects seen in a growing number of oncological pathologies, traumatic bone lesions, and revision surgeries.[3] Although cancer and trauma patients benefit from patient-specific implant designs, their chances of developing an IAI are increased because of their compromised immune system and the large open wounds, respectively.[4,5] Not surprisingly, because of existing bone-ingrowth around implants, revision surgeries are often complicated. To reduce this infection burden, we sought to develop a versatile coating technology that can deliver antibiotics locally and is also applicable on customized implants.[6]

Electrophoretic deposition (EPD) is a rapid and cost-effective coating method when compared to solvent casting,[7,8] layer-by-layer deposition,[9,10] and plasma-based coatings.[11,12] It is a site-selective and versatile technique that yields a uniform and stable coating with tunable thickness at room temperature.[13,14] We sought to combine this with additive manufacturing (AM) or 3D printing technology, as recent progress has enabled us to fabricate geometrically complex, porous, patient-specific implants to be used in complex orthopedic surgeries.[15,16] This approach will lead to better translation into clinical applications than traditional testing of biofunctionalized simple designs such as disk, rectangular, or rod-shaped samples,[17−19] because (1) the procedure yields the desired biofunctionality constantly (reproducibility) and (2) it is applicable to the real size implants (scalability).

Inspired by knee and hip implant designs, here we have developed two different 3D-printed samples, namely, cone and stem (Figure 1a). They were printed by selective laser melting (SLM) as AM technology (Figure 1b), followed by shot blasting treatment to get rid of the unmelted but attached powders on implant surfaces (Figure 1c). Finally, the samples underwent EPD coating to apply an antibacterial coating consisting of a chitosan/gelatin (Chi/Gel) hydrogel and two different antibiotics, vancomycin (Van) and gentamicin (Gen). Gentamicin and vancomycin are glycopeptide antibiotics with hydrophilic properties. The positively charged vancomycin and highly positively charged gentamicin form hydrogen and electrostatic bonds with the negatively charged gelatin, which ensures that particles of Chi/Gel loaded with antibiotics will be formed in the colloid solution.[20,21]

The detailed geometrical and morphological design parameters for the stem and cone samples are given in Table S1. After

Received: May 8, 2020
Accepted: September 7, 2020
Published: September 7, 2020

https://dx.doi.org/10.1021/acsbiomaterials.0c00683
ACS Biomater. Sci. Eng. 2020, 6, 5486−5492

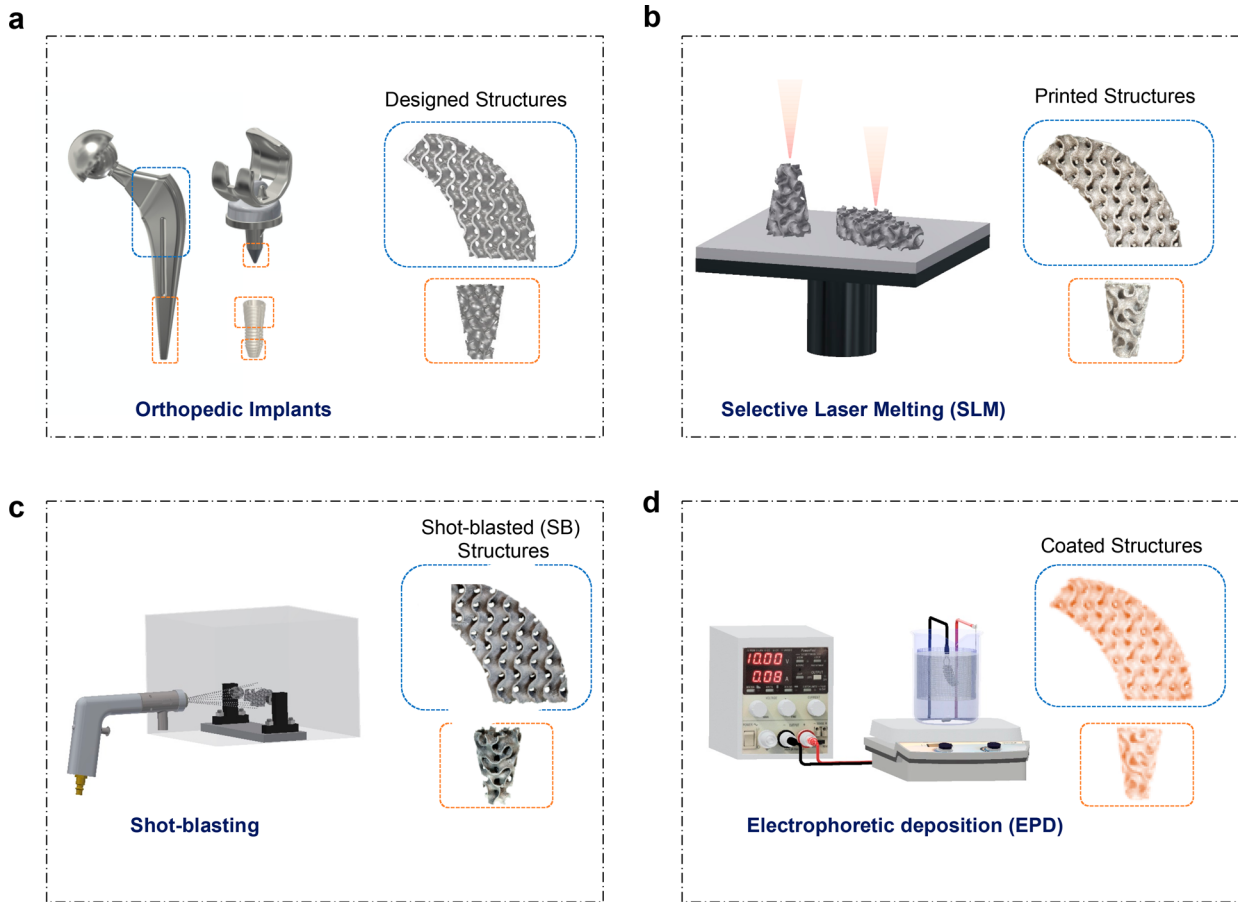

Figure 1. Illustration of printing and coating of complex implants (i.e., stem and cone-shaped). (a) Designing complex implants that mimic the real orthopedic implant. (b) Printing implants by selective laser melting (SLM) based on its design. (c) Shot blasting implants to eliminate the imperfections from implant surfaces. (d) Antibiotic coating of implants by the electrophoretic deposition (EPD) method.

the 3D printing, scanning electron microscopy (SEM) was used to show the surface morphology of the nonshot-blasted (NSB) and shot-blasted (SB) implant surfaces (Figure 2a). The SEM images clearly illustrated two different microstructures in cone and stem specimens, where the excessive powders were totally removed by SB but untouched in NSB samples. To apply a consistent and uniform coating on different implants, we performed an extensive optimization study in which the effects of time, voltage, and H_2O_2 were evaluated (Table S2). Fluorescein isothiocyanate (FITC) dye was included in Chi/Gel coatings to image the homogenicty of the coatings on implants using a fluorescent microscope (Figure S1). Fluorescent images also showed that the addition of H_2O_2 in the colloidal EPD solution led to more homogeneous coating, probably due to a reduction in bubble formation during EPD, in both stem and cone samples (Figure S2a) with and without shot blasting (Figure S2b). EDS mapping showed a highly increased elemental composition of carbon for all coated samples, (Table S3 and Figure S3). However, no increase in nitrogen and oxygen composition was observed for all coated samples compared to noncoated. The coated samples also showed a considerable decrease in the titanium and aluminum elements that exist in the titanium samples. The release profiles clearly showed the burst release of Van and Gen after 1 day (Figure 2c, d), which is followed by a small release during the next 7 days. The results showed that Van release for both stem and cone in SB implants was higher than NSB. Obviously, the stem samples showed a slightly higher release of vancomycin compared to the cone samples because of their larger surface area. On the other hand, the difference in the release of Gen in the NSB and SB samples was almost negligible and the amount of release for both stem and cone specimens was comparable. The micro roughness measurements confirmed that shot blasting were successful in elimination of unmelted Ti powder from the surface of implants (Figure 2e). All roughness parameters (including S_a, S_q, S_p, and S_v) showed remarkable differences between SB and NSB implants, as well as coated and noncoated implants (Figure 2e). However, there is a clear difference in the roughness of SB implants before and after the EPD coating because the coating on less-rough surfaces are more uniform and led to a more homogeneous coating.[22]

After we established the chemical specifics of our coating, we tested its antimicrobial properties. The number of adherent bacteria was significantly reduced (i.e., 2 log differences) in groups containing Van and Gen compared to Chi/Gel and As-Manufactured (AsM) groups at day 1 in both stem and cone samples (Figure 3a, d). Moreover, the antibiotics-containing coatings showed total eradication of nonadherent bacteria (i.e., planktonic bacteria) at day 1. The CFU results at day 7 showed no significant difference between experimental groups for both adherent and planktonic bacteria, neither between cone and stem samples nor between NSB or SB groups. The inhibition zone tests clearly showed a bactericidal potency of antibiotic-coated implants and thereby confirmed the CFU results at day 1 (Figure 3c, f).

https://dx.doi.org/10.1021/acsbiomaterials.0c00683
ACS Biomater. Sci. Eng. 2020, 6, 5486−5492

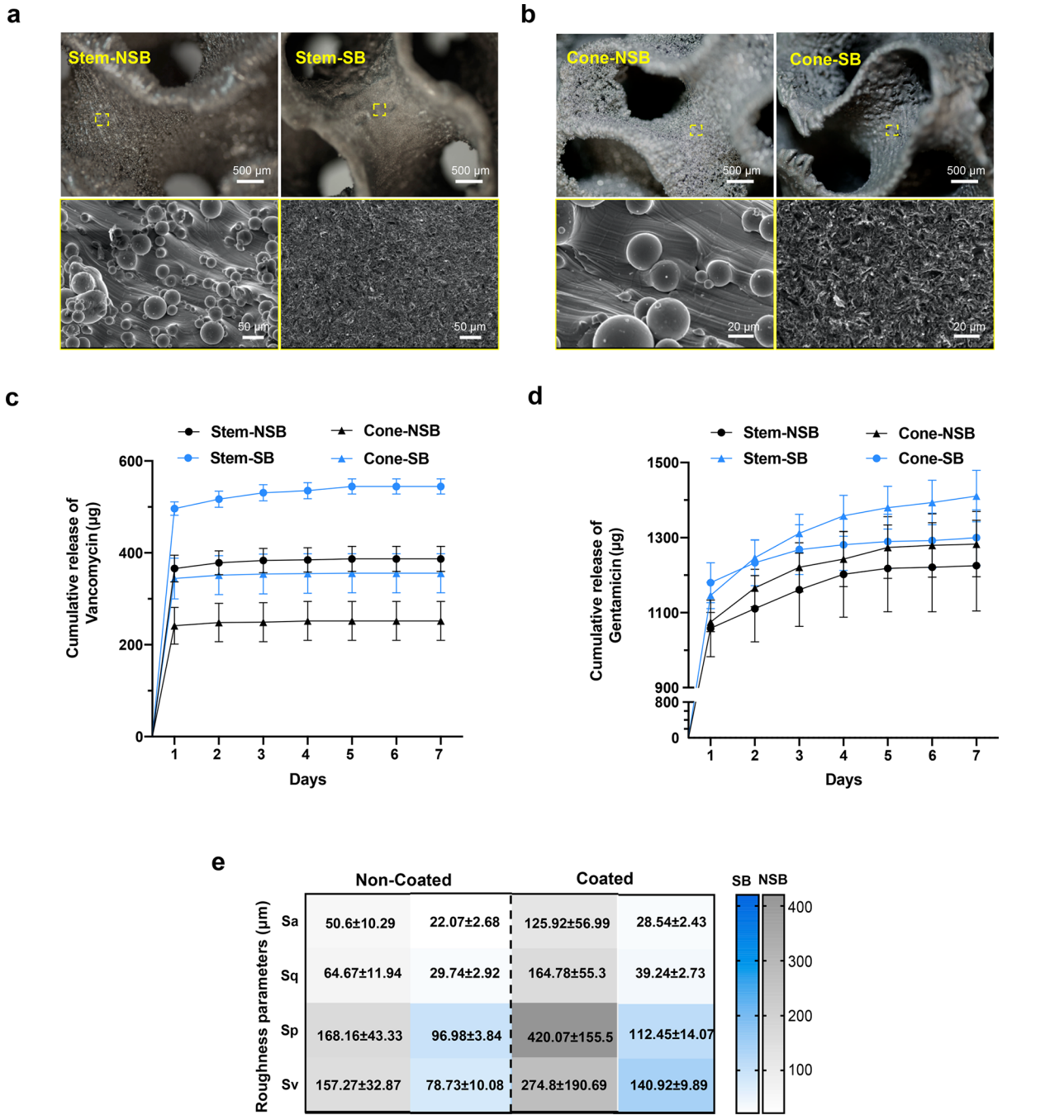

Figure 2. Characterization of additively manufactured shot-blasted (SB) and nonshot-blasted (NSB) implants. (a) SEM images of the SB and NSB stem implants. (b) SEM images of the SB and NSB cone implants. (c, d) Cumulative release of (c) vancomycin and (d) gentamicin from all antibiotic-included coatings for the SB and NSB stem and cone implants. Data are represented as the mean ± SD. (e) Roughness parameters of the SB and NSB stem implants before and after coating. Background color also reflects the values.

The Alamar blue assay showed no significant differences in metabolic activity of coated and noncoated groups for NSB structures of both cone and stem implants (Figure 4a, b). However, significant differences were observed between SB implants that were either coated or noncoated at day 1 and 3. DNA content also verified the results of alamar blue activity on stem and cone samples after 3 days (Figure 4c, d).

Host cells grown on noncoated implants showed higher metabolic activity than on coated implants. The live/dead staining showed no dead cells at day 3, which means that neither the coating polymer nor the antibiotics had any cytotoxic effect (Figure 4e). Altogether, this shows that our 3D printed, antibiotic-coated implants are antibacterial and biocompatible. The cytoskeleton staining showed different actin organization on NSB and SB structures at day 7 and 14 (Figure 4f, g). The more rounded actin organization was found on the NSB structure; however, the cells on the SB structure were more elongated and spread more on this structure than NSB.

DISCUSSIONS

Currently, healthcare is shifting its attention to personalized solutions and higher quality of care in terms of safety and

https://dx.doi.org/10.1021/acsbiomaterials.0c00683
ACS Biomater. Sci. Eng. 2020, 6, 5486−5492

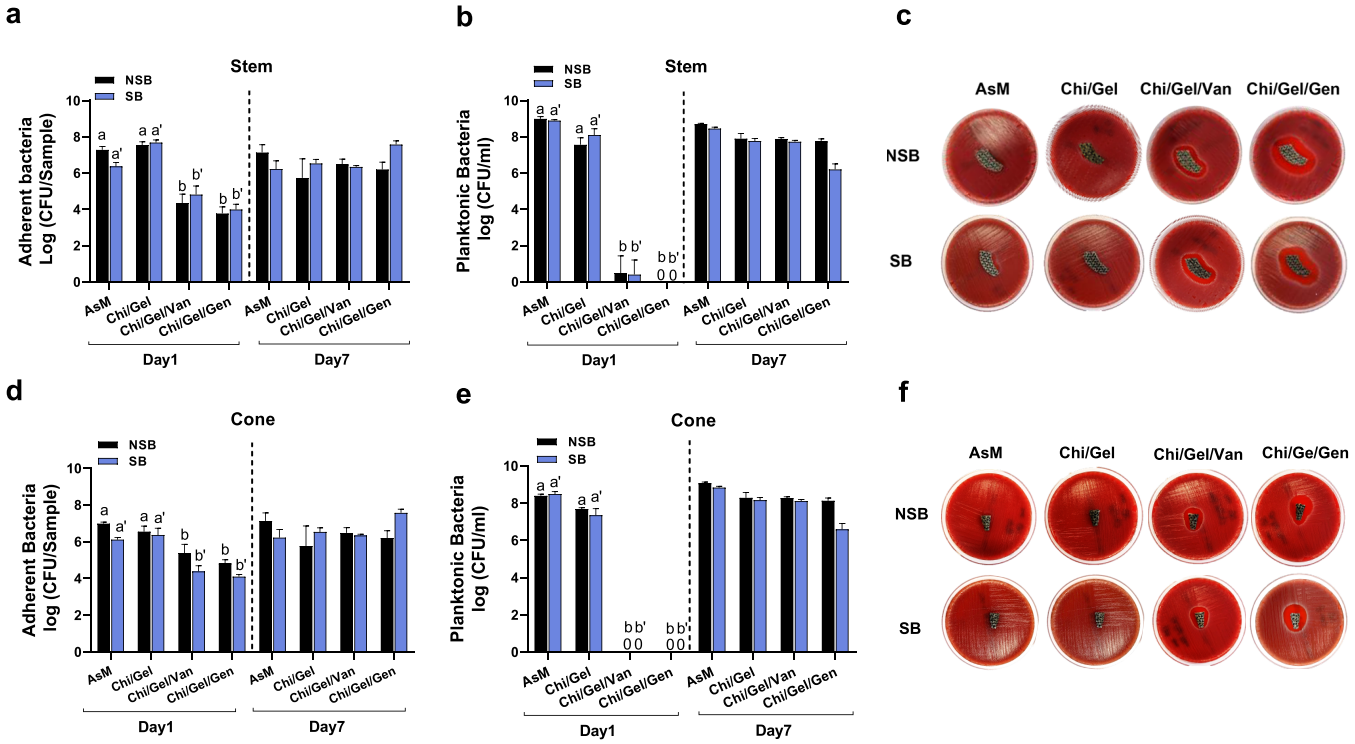

Figure 3. Antibacterial behavior of all antibiotic-containing coatings on SB and NSB implants. (a, b) Quantification of CFU surviving 24 h incubation with antibiotics released from stem implants. (c) Bacterial growth inhibition after 24 h on stem implants. (d, e) Quantification of CFU surviving 24 h incubation with antibiotics released from cone implants. (f) Bacterial growth inhibition after 24 h on cone implants. Data are represented as the mean ± SD ($P < 0.05$; a with b, a′, with b′, and no significant differences was observed between SB and NSB).

effectiveness.[23] Although patient-specific implants have been emerging on the market in the past decade, the invasive and complex nature of the related surgeries considerably increases the risk for infection.[24] Thus, applying bactericidal coatings on these personalized implants via a versatile technology could facilitate the right care for the right patient with maximum treatment effect and minimum side-effects and costs.

Adjusting the coating parameters to deliver a homogeneous and uniform coating on the entire 3D structure is very crucial for complex or 3D-printed implants. Here, the EPD technique was used because it allows for extreme control on particle size and morphology as well as coating thickness and uniformity.[25] One of its major advantages is that it is possible to add a variety of antibacterial agents (such as antibiotics and nanoparticles) by simply incorporating them into the different hydrogels.[26,27] Here, polyelectrolyte complexes of chitosan and gelatin could be formed by means of electrostatic interaction of the cationic amino groups of chitosan and the carboxilic group in gelatin, forming insoluble complexes that can be easily deposited on titanium surfaces.[25] Moreover, addition of hydrogen peroxide (H_2O_2) to the colloidal solution of EPD showed a better coating homogeneity (Figure S3b). Because of electrolysis during the EPD process, H_2 bubbles were formed at the cathodic side ($2H_2O > 2H_2 + O_2$).[28] Therefore, H_2O_2 could decrease this bubble formation and increase homogeneity. The excessive bubble formation at the cathodic side could lead to non-homogenous coating structure. To maximize the homogentiy and quality of the coating, researchers have used different mechanical and chemical surface treatments to remove the excessive powder of 3D-printed titanium implants.[29,30] Traditionally, surface mechanical treatment such as shot blasting has also been used to induce a compressive residual stress layer on implants and thereby prevent fatigue crack propagation.[31] Nevertheless, it is also useful to reduce bacterial adherence and improve tissue regenerations of implants.[32,33] In line with the previous findings, the shot blasted samples not only altered the release kinetics of antibiotics and antibacterial properties against planktonic bacteria, but also yielded more organized and orientated cells than non-treated samples, which could modulate cell spreading to promote implant integration into the bone.[34−36]

The advantage of our new coating strategy is 2-fold: (1) it can be combined with 3D-printed personalized implants, and (2) it assures local release of high concentrations of antibiotics near the implant. Especially for this high concentration, local release is important, because it will lower the systemic adverse affects of the antibiotic despite reaching therapeutic concentrations at the infection site. Furthermore, it will have a high chance of killing all planktonic bacteria for up to 24 h, thus limiting the selection of antibiotic-resistant clones at the infection site. Although we have now tested the incorporation of two different antibiotics (i.e., gentamicin and vancomycin), EPD also allows for incorporation of other antibiotics. This would provide the additional benefit of tailoring the antibiotic treatment to the antibiotic susceptibility of the infecting bacterial strain.

We showed the potency of our implants in vitro, but to facilitate their clinical appreciation, future in vivo evaluation must be carefully planned. In vivo models should be able to mimic complex bone and nonhealing bone defects that can be treated with patient-specific (porous), load-bearing implants, which are prone to bacterial contamination.[37]

https://dx.doi.org/10.1021/acsbiomaterials.0c00683
ACS Biomater. Sci. Eng. 2020, 6, 5486−5492

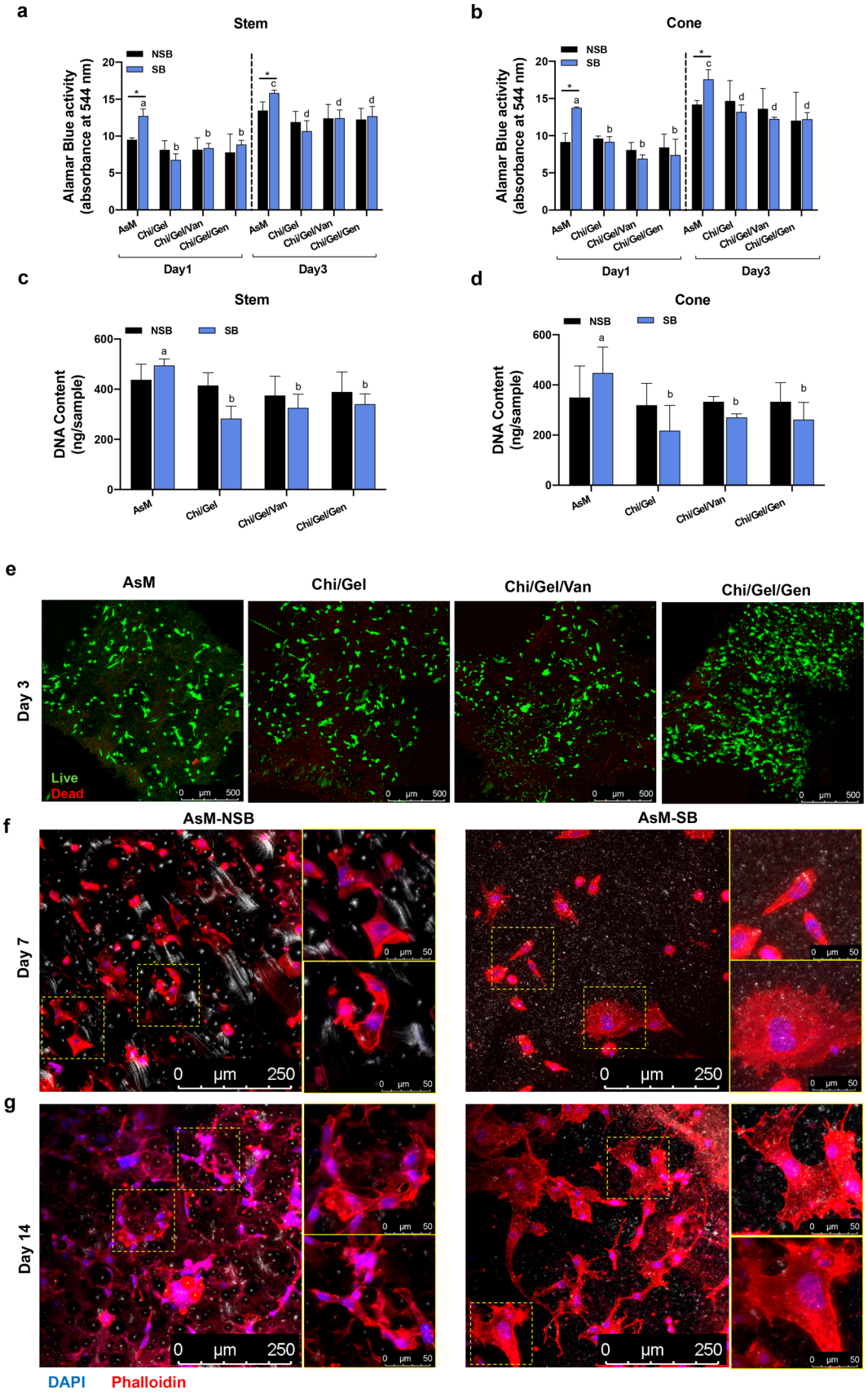

Figure 4. Osteoblast precursor cell behavior of all antibiotic-containing coatings on SB and NSB Stem implants. (a, b) Alamar blue activity of the cells on implants after 1 and 3 days. (c, d) DNA content of the cells on implants after 3 days. (e) Live−dead staining of cells on stem samples after 3 days (live, green; dead, red). (f, g) Cytoskeleton staining of cells on stem samples after 7 and 14 days (DAPI, blue; phalloidin, red). Data are represented as the mean ± SD ($P < 0.05$; a with b, c with d, and * shows the significant differences between SB and NSB).

https://dx.doi.org/10.1021/acsbiomaterials.0c00683
ACS Biomater. Sci. Eng. 2020, 6, 5486−5492

CONCLUSIONS

A chitosan/gelatin composite coating loaded with antibiotics was successfully deposited on complex, 3D-printed implants by means of EPD. All groups showed a stable and uniform coating on the additively manufactured complex titanium implants. A burst release of antibiotics resulted in high degradability of the coating due to the gelatin incorporation in the particle complexes. A difference in the surface roughness did not significantly affect coating deposition, release behavior, cell proliferation, or antibacterial activity. Importantly, around all coated implants that contained antibiotics, the number of the planktonic and adherent bacteria tremendously decreased within 24 h. Collectively, the findings of this study pave the way toward antibacterial coating for personalized implants.

ASSOCIATED CONTENT

Supporting Information

The Supporting Information is available free of charge at https://pubs.acs.org/doi/10.1021/acsbiomaterials.0c00683.

Materials and methods, geometrical and morphological design parameters for the stem and cone samples, EPD parameter optimization for different groups, chemical composition of all experimental groups measured at a representative area (PDF)

AUTHOR INFORMATION

Corresponding Author

S. Amin Yavari − *Department of Orthopedics, University Medical Center Utrecht, Utrecht 3584 CX, The Netherlands;* orcid.org/0000-0003-1677-5751; Phone: +31 (0)88 75 56481; Email: S.AminYavari@umcutrecht.nl, saber.aminyavari@gmail.com; Fax: +31 (0)30 25 106 38

Authors

F. Jahanmard − *Department of Orthopedics, University Medical Center Utrecht, Utrecht 3584 CX, The Netherlands*

F.M. Dijkmans − *Department of Orthopedics, University Medical Center Utrecht, Utrecht 3584 CX, The Netherlands*

A. Majed − *Department of Orthopedics, University Medical Center Utrecht, Utrecht 3584 CX, The Netherlands*

H.C. Vogely − *Department of Orthopedics, University Medical Center Utrecht, Utrecht 3584 CX, The Netherlands*

B.C.H. van der Wal − *Department of Orthopedics, University Medical Center Utrecht, Utrecht 3584 CX, The Netherlands*

D.A.C. Stapels − *Department of Medical Microbiology, University Medical Center Utrecht, Utrecht 3584 CX, The Netherlands*

S.M. Ahmadi − *Amber Implants B.V., Delft 2629 JD, The Netherlands*

T. Vermonden − *Department of Pharmaceutics, Utrecht Institute for Pharmaceutical Sciences (UIPS), Utrecht University, Utrecht 3584 CS, The Netherlands;* orcid.org/0000-0002-6047-5900

Complete contact information is available at: https://pubs.acs.org/10.1021/acsbiomaterials.0c00683

Author Contributions

†F.J. and F.M.D. contributed equally to this work.

Notes

The authors declare no competing financial interest.

ACKNOWLEDGMENTS

The collaboration project is cofunded by the PPP Allowance made available by Health~Holland, Top Sector Life Sciences & Health, to stimulate public-private partnerships.

REFERENCES

(1) Costerton, J. W.; Stewart, P. S.; Greenberg, E. P. Bacterial biofilms: a common cause of persistent infections. *Science* **1999**, *284* (5418), 1318−1322.

(2) Ceri, H.; Olson, M.; Stremick, C.; Read, R.; Morck, D.; Buret, A. The Calgary Biofilm Device: new technology for rapid determination of antibiotic susceptibilities of bacterial biofilms. *J. Clin. Microbiol.* **1999**, *37* (6), 1771−1776.

(3) Willemsen, K.; Nizak, R.; Noordmans, H. J.; Castelein, R. M.; Weinans, H.; Kruyt, M. C. Challenges in the design and regulatory approval of 3D-printed surgical implants: a two-case series. *Lancet Digital Health* **2019**, *1* (4), e163−e171.

(4) Rolston, K. V. Infections in cancer patients with solid tumors: a review. *Infect Dis Ther* **2017**, *6* (1), 69−83.

(5) Zajonz, D.; Birke, U.; Ghanem, M.; Prietzel, T.; Josten, C.; Roth, A.; Fakler, J. K. M. Silver-coated modular Megaendoprostheses in salvage revision arthroplasty after periimplant infection with extensive bone loss − a pilot study of 34 patients. *BMC Musculoskeletal Disord.* **2017**, *18* (1), 383.

(6) Zhang, K.; Wang, S.; Zhou, C.; Cheng, L.; Gao, X.; Xie, X.; Sun, J.; Wang, H.; Weir, M. D.; Reynolds, M. A.; Zhang, N.; Bai, Y.; Xu, H. H. K. Advanced smart biomaterials and constructs for hard tissue engineering and regeneration. *Bone Res.* **2018**, *6* (1), 31.

(7) Mishra, S. K.; Ferreira, J. M. F.; Kannan, S. Mechanically stable antimicrobial chitosan−PVA−silver nanocomposite coatings deposited on titanium implants. *Carbohydr. Polym.* **2015**, *121*, 37−48.

(8) Bayer, I. S.; Fragouli, D.; Attanasio, A.; Sorce, B.; Bertoni, G.; Brescia, R.; Di Corato, R.; Pellegrino, T.; Kalyva, M.; Sabella, S.; Pompa, P. P.; Cingolani, R.; Athanassiou, A. Water-Repellent Cellulose Fiber Networks with Multifunctional Properties. *ACS Appl. Mater. Interfaces* **2011**, *3* (10), 4024−4031.

(9) Borkner, C. B.; Wohlrab, S.; Möller, E.; Lang, G.; Scheibel, T. Surface Modification of Polymeric Biomaterials Using Recombinant Spider Silk Proteins. *ACS Biomater. Sci. Eng.* **2017**, *3* (5), 767−775.

(10) Amin Yavari, S.; Croes, M.; Akhavan, B.; Jahanmard, F.; Eigenhuis, C. C.; Dadbakhsh, S.; Vogely, H. C.; Bilek, M. M.; Fluit, A. C.; Boel, C. H. E.; van der Wal, B. C. H.; Vermonden, T.; Weinans, H.; Zadpoor, A. A. Layer by layer coating for bio-functionalization of additively manufactured meta-biomaterials. *Addit. Manuf.* **2020**, *32*, 100991.

(11) Peng, F.; Wang, D.; Zhang, D.; Yan, B.; Cao, H.; Qiao, Y.; Liu, X. PEO/Mg−Zn−Al LDH Composite Coating on Mg Alloy as a Zn/Mg Ion-Release Platform with Multifunctions: Enhanced Corrosion Resistance, Osteogenic, and Antibacterial Activities. *ACS Biomater. Sci. Eng.* **2018**, *4* (12), 4112−4121.

(12) Akhavan, B.; Bakhshandeh, S.; Najafi-Ashtiani, H.; Fluit, A. C.; Boel, E.; Vogely, C.; van der Wal, B. C. H.; Zadpoor, A. A.; Weinans, H.; Hennink, W. E.; Bilek, M. M.; Amin Yavari, S. Direct covalent attachment of silver nanoparticles on radical-rich plasma polymer films for antibacterial applications. *J. Mater. Chem. B* **2018**, *6* (37), 5845−5853.

(13) Stevanović, M.; Đošić, M.; Janković, A.; Kojić, V.; Vukašinović-Sekulić, M.; Stojanović, J.; Odović, J.; Crevar Sakač, M.; Rhee, K. Y.; Mišković-Stanković, V. Gentamicin-Loaded Bioactive Hydroxyapatite/Chitosan Composite Coating Electrodeposited on Titanium. *ACS Biomater. Sci. Eng.* **2018**, *4* (12), 3994−4007.

(14) Bakhshandeh, S.; Amin Yavari, S. Electrophoretic deposition: a versatile tool against biomaterial associated infections. *J. Mater. Chem. B* **2018**, *6* (8), 1128−1148.

(15) Zadpoor, A. A.; Malda, J. Additive Manufacturing of Biomaterials, Tissues, and Organs. *Ann. Biomed. Eng.* **2017**, *45* (1), 1−11.

(16) Hollister, S. J.; Flanagan, C. L.; Morrison, R. J.; Patel, J. J.; Wheeler, M. B.; Edwards, S. P.; Green, G. E. Integrating Image-Based Design and 3D Biomaterial Printing To Create Patient Specific Devices within a Design Control Framework for Clinical Translation. *ACS Biomater. Sci. Eng.* **2016**, *2* (10), 1827−1836.
(17) Bakhshandeh, S.; Gorgin Karaji, Z.; Lietaert, K.; Fluit, A. C.; Boel, C. H. E.; Vogely, H. C.; Vermonden, T.; Hennink, W. E.; Weinans, H.; Zadpoor, A. A.; Amin Yavari, S. Simultaneous Delivery of Multiple Antibacterial Agents from Additively Manufactured Porous Biomaterials to Fully Eradicate Planktonic and Adherent Staphylococcus aureus. *ACS Appl. Mater. Interfaces* **2017**, *9* (31), 25691−25699.
(18) Croes, M.; Bakhshandeh, S.; van Hengel, I. A. J.; Lietaert, K.; van Kessel, K. P. M.; Pouran, B.; van der Wal, B. C. H.; Vogely, H. C.; Van Hecke, W.; Fluit, A. C.; Boel, C. H. E.; Alblas, J.; Zadpoor, A. A.; Weinans, H.; Amin Yavari, S. Antibacterial and immunogenic behavior of silver coatings on additively manufactured porous titanium. *Acta Biomater.* **2018**, *81*, 315−327.
(19) Van Der Stok, J.; Lozano, D.; Chai, Y. C.; Amin Yavari, S.; Bastidas Coral, A. P.; Verhaar, J. A.; Gómez-Barrena, E.; Schrooten, J.; Jahr, H.; Zadpoor, A. A.; et al. Osteostatin-coated porous titanium can improve early bone regeneration of cortical bone defects in rats. *Tissue Eng., Part A* **2015**, *21* (9−10), 1495−1506.
(20) Song, J.; Odekerken, J. C.; Löwik, D. W.; López-Pérez, P. M.; Welting, T. J.; Yang, F.; Jansen, J. A.; Leeuwenburgh, S. C. Influence of the molecular weight and charge of antibiotics on their release kinetics from gelatin nanospheres. *Macromol. Biosci.* **2015**, *15* (7), 901−911.
(21) Ahangari, A.; Salouti, M.; Heidari, Z.; Kazemizadeh, A. R.; Safari, A. A. Development of gentamicin-gold nanospheres for antimicrobial drug delivery to Staphylococcal infected foci. *Drug Delivery* **2013**, *20* (1), 34−39.
(22) Li, J.; Du, A.; Fan, Y.; Zhao, X.; Ma, R.; Wu, J. Effect of shot-blasting pretreatment on microstructures of hot-dip galvanized coating. *Surf. Coat. Technol.* **2019**, *364*, 218−224.
(23) Lewy, H.; Barkan, R.; Sela, T., Personalized Health Systems—Past, Present, and Future of Research Development and Implementation in Real-Life Environment. *Front. Med.* **2019**, *6* (149), DOI: 10.3389/fmed.2019.00149.
(24) Wafa, H.; Grimer, R.; Reddy, K.; Jeys, L.; Abudu, A.; Carter, S.; Tillman, R. Retrospective evaluation of the incidence of early periprosthetic infection with silver-treated endoprostheses in high-risk patients: case-control study. *Bone Jt. J.* **2015**, *97* (2), 252−257.
(25) Avcu, E.; Baştan, F. E.; Abdullah, H. Z.; Rehman, M. A. U.; Avcu, Y. Y.; Boccaccini, A. R. Electrophoretic deposition of chitosan-based composite coatings for biomedical applications: A review. *Prog. Mater. Sci.* **2019**, *103*, 69−108.
(26) Seuss, S.; Boccaccini, A. R. Electrophoretic Deposition of Biological Macromolecules, Drugs, And Cells. *Biomacromolecules* **2013**, *14* (10), 3355−3369.
(27) Li, M.; Chen, Q.; Ma, M.; Liu, X.; Dong, K.; Zhang, Y.; Lu, T. Electrophoretic deposition of core-shell Ag@MSN incorporated-chitosan coatings with biocompatible and antibacterial activities. *Mater. Lett.* **2019**, *239*, 29−32.
(28) Wang, Y.; Guo, X.; Pan, R.; Han, D.; Chen, T.; Geng, Z.; Xiong, Y.; Chen, Y. Electrodeposition of chitosan/gelatin/nanosilver: A new method for constructing biopolymer/nanoparticle composite films with conductivity and antibacterial activity. *Mater. Sci. Eng., C* **2015**, *53*, 222−228.
(29) Pyka, G.; Burakowski, A.; Kerckhofs, G.; Moesen, M.; Van Bael, S.; Schrooten, J.; Wevers, M. Surface Modification of Ti6Al4V Open Porous Structures Produced by Additive Manufacturing. *Adv. Eng. Mater.* **2012**, *14* (6), 363−370.
(30) Persenot, T.; Burr, A.; Plancher, E.; Buffière, J.-Y.; Dendievel, R.; Martin, G. Effect of ultrasonic shot peening on the surface defects of thin struts built by electron beam melting: Consequences on fatigue resistance. *Addit. Manuf.* **2019**, *28*, 821−830.
(31) Bagherifard, S. Enhancing the Structural Performance of Lightweight Metals by Shot Peening. *Adv. Eng. Mater.* **2019**, *21* (7), 1801140.
(32) Bagherifard, S.; Hickey, D. J.; de Luca, A. C.; Malheiro, V. N.; Markaki, A. E.; Guagliano, M.; Webster, T. J. The influence of nanostructured features on bacterial adhesion and bone cell functions on severely shot peened 316L stainless steel. *Biomaterials* **2015**, *73*, 185−197.
(33) Jang, Y.; Choi, W. T.; Johnson, C. T.; García, A. J.; Singh, P. M.; Breedveld, V.; Hess, D. W.; Champion, J. A. Inhibition of Bacterial Adhesion on Nanotextured Stainless Steel 316L by Electrochemical Etching. *ACS Biomater. Sci. Eng.* **2018**, *4* (1), 90−97.
(34) Yin, F.; Xu, R.; Hu, S.; Zhao, K.; Yang, S.; Kuang, S.; Li, Q.; Han, Q. Enhanced Mechanical and Biological Performance of an Extremely Fine Nanograined 316L Stainless Steel Cell−Substrate Interface Fabricated by Ultrasonic Shot Peening. *ACS Biomater. Sci. Eng.* **2018**, *4* (5), 1609−1621.
(35) Truong, V. K.; Lapovok, R.; Estrin, Y. S.; Rundell, S.; Wang, J. Y.; Fluke, C. J.; Crawford, R. J.; Ivanova, E. P. The influence of nano-scale surface roughness on bacterial adhesion to ultrafine-grained titanium. *Biomaterials* **2010**, *31* (13), 3674−3683.
(36) Wu, Y.; Zitelli, J. P.; TenHuisen, K. S.; Yu, X.; Libera, M. R. Differential response of Staphylococci and osteoblasts to varying titanium surface roughness. *Biomaterials* **2011**, *32* (4), 951−960.
(37) Busscher, H. J.; Woudstra, W.; van Kooten, T. G.; Jutte, P.; Shi, L.; Liu, J.; Hinrichs, W. L. J.; Frijlink, H. W.; Shi, R.; Liu, J.; Parvizi, J.; Kates, S.; Rotello, V. M.; Schaer, T. P.; Williams, D.; Grainger, D. W.; van der Mei, H. C. Accepting higher morbidity in exchange for sacrificing fewer animals in studies developing novel infection-control strategies. *Biomaterials* **2020**, *232*, 119737.

https://dx.doi.org/10.1021/acsbiomaterials.0c00683
ACS Biomater. Sci. Eng. 2020, 6, 5486−5492